

# Three-dimensional matter-wave vortices in optical lattices

Tristram J. Alexander, Elena A. Ostrovskaya, Andrey A. Sukhorukov, and Yuri S. Kivshar  
Nonlinear Physics Centre and Australian Centre of Excellence for Quantum Atom Optics,  
Research School of Physical Sciences and Engineering,  
Australian National University, Canberra, ACT 0200, Australia

We predict the existence of spatially localized nontrivial vortex states of a Bose-Einstein condensate with repulsive atomic interaction confined by a three-dimensional optical lattice. Such vortex-like structures include planar vortices, their co- and counter-rotating bound states, and distinctly three-dimensional non-planar vortex states. We demonstrate numerically that many of these vortex structures are remarkably robust, and therefore can be generated and observed in experiment.

PACS numbers: 03.75.Lm

The importance of three-dimensional (3D) vortex configurations in physics was recognized long ago by Sir W. Thompson when he suggested that robust vortex rings can be employed to understand the structure of the atom [1]. Since then topologically stable vortex lines have been investigated in many physical contexts, including cosmology, hydrodynamics, optics, and condensed matter physics. New experimental opportunities for the study of vortices have appeared in the rapidly developing field of Bose-Einstein condensates (BECs) [2] as condensates provide an excellent test system for the study of nucleation, dynamics, and the interaction of vortex lines.

One of the outstanding physical problems is the behavior of vortices in systems with reduced symmetry, such as periodic structures. BECs loaded into periodic potentials of optical lattices provide an excellent example of such a system, being relatively easy to manipulate experimentally. In a two-dimensional (2D) geometry, stable vortices localized in an optical lattice were predicted to exist in the form of matter-wave gap vortices [3]. These vortices are spatially localized states of the condensate with a phase circulation that exist due to the interplay of the repulsive nonlinearity and the anomalous diffraction of the matter waves due to their Bragg scattering in the lattice. Although 2D (planar) vortices have also been investigated in 3D discrete lattice models [4], nothing is known about nonlinear dynamics of the vortex states in a fully 3D continuous lattice geometry.

In this Letter we not only show that planar 2D matter-wave gap vortices persist in the presence of the third lattice dimension, but also predict the existence of completely new vortex states localized inside the lattice. In particular we show that the circulation of particles can break the traditional 2D vortex symmetry and form states which circulate simultaneously in multiple symmetry planes. Furthermore we show that the 3D lattice provides a unique opportunity to study the coherent interaction of multiple vortices, and demonstrate that an interacting stack of vortices containing an extended vortex line, which is known to be unstable in homogeneous systems, is stabilized by the lattice. As 3D optical lattices provide improved control over condensate excita-

tions [5], there is promise for the future experimental study of these highly nontrivial vortex phenomena.

We model the macroscopic dynamics of the Bose-Einstein condensate in a 3D optical lattice by the rescaled mean-field Gross-Pitaevskii (GP) equation:

$$i\frac{\partial \psi}{\partial t} + \frac{1}{2} \nabla^2 \psi + V(\mathbf{r}) \psi + |\psi|^2 \psi = 0; \quad (1)$$

where  $\psi$  is the complex matter-wave wavefunction,  $\mathbf{r} = (x; y; z)$ ,  $\nabla^2 = \partial^2/\partial x^2 + \partial^2/\partial y^2 + \partial^2/\partial z^2$ , and  $\mu = 1$  for repulsive atomic interactions. The characteristic spatial scale is  $a_L = d/\lambda$ , where  $d = 2\pi/\lambda$  is the lattice period, and  $\lambda$  is the wavelength of the light producing the lattice. We consider a cubic lattice potential:

$$V(\mathbf{r}) = V_0 (\sin^2 x + \sin^2 y + \sin^2 z); \quad (2)$$

with the depth  $V_0$  scaled by the lattice recoil energy  $E_L = \hbar^2/(2m a_L^2)$ . The characteristic time scale is given by  $\tau_L = \hbar/E_L$ . We have neglected any additional trapping potential as we are interested in spatial localization due to the optical lattice and nonlinearity.

We look for the stationary solutions of Eq. (1) using the ansatz  $\psi(\mathbf{r}; t) = \psi(\mathbf{r}) \exp(-i\mu t)$ , where  $\mu$  is the chemical potential. At low atomic densities, the condensate dynamics in the lattice is described by the linearized Eq. (1) where the last term is neglected. Due to the periodicity of the potential, the corresponding stationary states can be expressed as a superposition of the Floquet-Bloch modes satisfying the condition,  $\psi_{\mathbf{k}}(\mathbf{r}) = B_{\mathbf{k}}(\mathbf{r}) \exp(i\mathbf{k} \cdot \mathbf{r})$ , where  $B_{\mathbf{k}}(\mathbf{r}) = B_{\mathbf{k}}(\mathbf{r} + \mathbf{d})$ , and  $\mathbf{k}$  is the quasimomentum within the first Brillouin zone of the lattice (see Fig. 1). Matter waves can propagate through the lattice if  $\mathbf{k}$  is real-valued, i.e. when the chemical potential of the Floquet-Bloch linear states belongs to one of the bands (shaded in Fig. 1). In the 3D potential (2), there always exists a semi-infinite spectral gap extending to  $\mu = 1$ , and additional gaps appear only when the potential depth  $V_0$  exceeds the threshold value  $V_{th} \approx 2.24$ . In what follows we choose the value  $V_0 = 6$ .

At higher atomic densities, the effect of repulsive atom-atom interactions described by the nonlinear term in

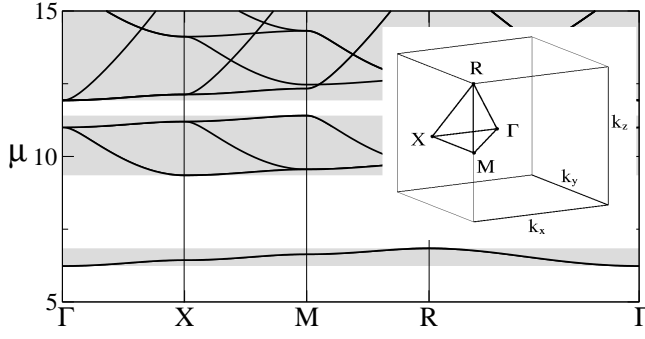


FIG. 1: Matter-wave spectrum  $\mu(\mathbf{k})$  in a three-dimensional optical lattice (2) at  $V_0 = 6$ . Shaded and open areas show bands and gaps, respectively. Inset shows the first Brillouin zone and the high-symmetry points in the reciprocal lattice.

Eq. (1) becomes important. In free space, repulsive non-linearity tends to accelerate the spreading of the condensate. However, in a lattice the effective mass of the condensate becomes negative near the lower gap edges [8], allowing for the formation of localized states inside the spectral gaps [6]. These nonlinear states – gap solitons – are localized in all three dimensions. Figure 2 shows an example of a gap soliton, and the dependence of its norm,  $N = \int |\psi|^2 d\mathbf{r}$ , on the chemical potential within the first gap calculated using a numerical functional minimization technique [7]. Despite a nontrivial phase of the wavefunction [see Fig. 2 (c)], characteristic of linear Bloch wave tails, there is no particle flow in the soliton.

Near the lower gap edge the soliton spreads over many lattice sites and may be described by the free-space GP equation for an envelope of the corresponding Bloch state [8]. In this limit, the 3D gap soliton is expected to be unstable according to the Vakhitov-Kolokolov criterion since  $dN/d\mu < 0$  [see Fig. 2 (a)]. Such an instability may result in the transformation of a weakly localized atomic cloud into a highly condensed state deeper inside the gap [such as shown in Fig. 2 (b,c)], where  $dN/d\mu > 0$ . We have investigated the dynamical stability of the strongly localized gap solitons numerically by introducing 5% random phase and amplitude perturbations. No evidence of instability can be seen over the evolution time  $t = 10^3$ , which for  $^{87}\text{Rb}$  in an optical lattice created with a 0.25  $\mu\text{m}$  period is equivalent to 17 ms.

Spatially localized stationary states of the repulsive condensate with a phase circulation can also exist in the gaps of the linear spectrum. These are localized vortices with stationary density distribution, but nonvanishing particle flow around a closed path, which can be characterized by the local current density,  $\mathbf{j} = 2\text{Im}(\psi^* \nabla \psi)$ . The gap vortex states in a lattice can be thought of as clusters of gap solitons  $\psi_s$  having different positions on the lattice  $\mathbf{r}_m$  and phases  $\theta_m$ . The vortex flow between such solitons occurs due to a nontrivial phase structure of the full matter-wave function which is approximately

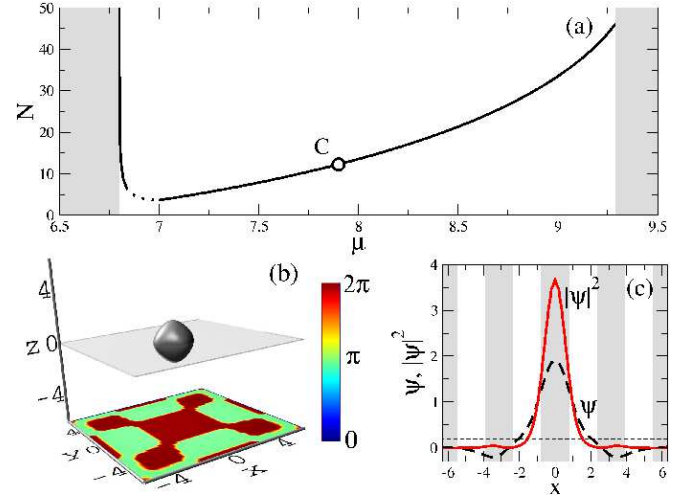


FIG. 2: (color online) Gap soliton in a 3D optical lattice with  $V_0 = 6$ . (a) Norm of the wavefunction  $N$  vs.  $\mu$  inside the gap; point C (at  $\mu = 7.9$ ) corresponds to the state shown in (b) and (c). Line at left band edge calculated in free-space GP limit. Dotted line an interpolation. (b) An isosurface of the soliton density,  $|\psi|^2$ , at the level  $|\psi|^2 = 0.2$ , with phase in the  $z = 0$  plane (semi-transparent) shown below. (c) The cuts of  $\psi$  (dashed) and  $|\psi|^2$  (solid) along the line  $y = z = 0$ . Thin dashed line corresponds to  $|\psi|^2 = 0.2$ . Shaded areas show the lattice minima (parts of the potential less than  $V_0 = 2$ ).

found as  $\psi = \sum_{m=1}^M \psi_s(\mathbf{r} - \mathbf{r}_m) \exp(i\theta_m)$ . Formation of a stationary vortex is possible when all the incoming and outgoing flows are balanced and hence [9]:

$$\sum_{m=1}^M c_{nm} \sin(\theta_m - \theta_n) = 0: \quad (3)$$

Each term in this sum denotes the flow between gap solitons numbered  $n$  and  $m$ , which depends on the relative phases and the nonlinear coupling constants  $c_{nm}$ .  $c_{nm} = \int \psi_s^3(\mathbf{r} - \mathbf{r}_n) \psi_s^2(\mathbf{r} - \mathbf{r}_m) d\mathbf{r} = \int \psi_s^5(\mathbf{r}) d\mathbf{r}$ .

The sign of the coupling depends on the sign of the overlap between the wavefunctions of the gap solitons and the sign of the nonlinearity. The former may be positive or negative due to the oscillating tails of the gap solitons [Fig. 2 (c)]. As the latter is negative ( $\gamma = -1$ ), positive coupling occurs when the overlapping parts of the wavefunctions are out-of-phase. Solitons in the cluster can be positioned in the “nearest neighbor” configuration, whereby they are separated by a single lattice period in the  $x$ ,  $y$  or  $z$  direction, or in a “next neighbor” configuration, whereby the solitons are placed in-plane, diagonally across a lattice cell (e.g. in the direction  $(1, 1, 1)$  in Fig. 1). The “nearest neighbor” coupling is positive, whereas the “next neighbor” coupling is negative. Importantly, for a positive coupling, the flow is directed from a soliton with phase  $\theta_m = 0$  to one with  $\theta = 2\pi$  etc., while for negative coupling the flow is reversed. Below we discuss the physical origins of this reversal.

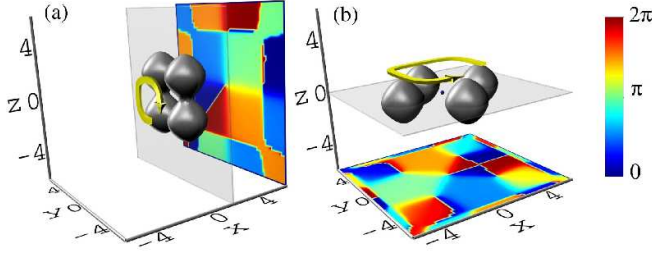


FIG. 3: (color online) Examples of planar (a) on-site and (b) off-site vortices ( $V_0 = 6$ ,  $\gamma = 7.9$ ). The orientation in (a) is the  $(x, y)$  plane, while in (b) it is the  $(y, z)$  plane. Arrows show directions of particle flow.

A 3D lattice can support vortex states of different geometries. First and the most obvious type are the gap vortices localized in a plane which can be considered as a generalization of 2D gap vortices [3]. Such 2D states were shown to have two basic symmetries relative to the lattice sites: on-site and off-site vortices [3]. The off-site vortex has a lattice maximum at its center and, therefore, it may consist of four lobes (atomic density maxima) in a nearest neighbor configuration [Fig. 3 (a)]. As the nearest neighbor coupling is positive, the flow circulation is defined in the direction  $0 \rightarrow 1 \rightarrow 2 \rightarrow 3 \rightarrow 0$  of the phases of the composite solitons. The on-site vortices are centered on a lattice site and consist of four lobes in the next neighbor configuration [Fig. 3 (b)]. With the nearest neighbor coupling normalized to +1, the on-site vortex has an inter-lobe next neighbor coupling of  $0:1:1$ , and the particle flow is opposite to that expected from the composite soliton phases. At the physical level, as particle flow is always directed along the phase gradient this seemingly anomalous flow actually arises through the interference of multiple phase singularities producing a counter-flow opposite to that of the central singularity.

We have examined the dynamical stability of the planar vortices shown in Figs. 3 (a,b) numerically and found that they are stable, at least up to  $t = 10^3$ . An important consequence of the 3D geometry is that we may orient these planar vortices in any of the three symmetry planes of the lattice. Additional planes exist in the three-dimensional lattice, however they are asymmetric with respect to the inter-site coupling, and we expect such planes to host asymmetric planar vortices [9].

A new feature of 3D optical lattices is the possibility of studying the coherent interaction of multiple planar vortices. From the analysis of the discrete equations (3), we have identified three basic types of coupled pairs of planar vortices: in-phase, out-of-phase, and hybrid-phase. These may be described by the phases of the vortex lobes. The in-phase pair has a phase structure, in multiples of  $\pi/2$ , corresponding to  $(0;0; \frac{1}{2}; \frac{1}{2}); (1;1; \frac{3}{2}; \frac{3}{2})$  where we have used the notation of  $[\text{vortex}_1; \text{vortex}_2]$  for each of the four lobes. The out-of-phase pair has a phase

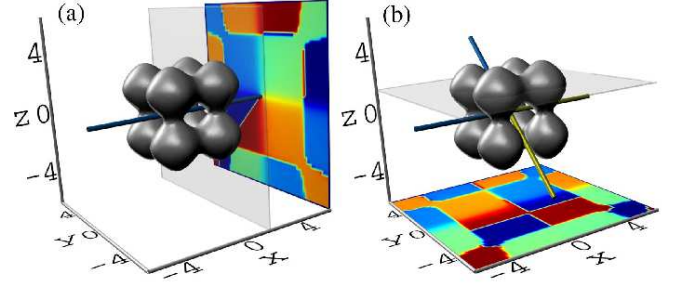


FIG. 4: (color online) Examples of interacting vortex solitons at  $V_0 = 6$ ,  $\gamma = 7.9$ . (a) In-phase co-rotating vortex pair. (b) Counter-rotating vortex pair. Lines correspond to primary vortex lines, with different shadings showing opposite topological charges.

of  $(0;1; \frac{1}{2}; \frac{3}{2}); (1;0; \frac{3}{2}; \frac{1}{2})$ , while the hybrid vortex pair has a phase structure  $(0;0; \frac{1}{2}; \frac{3}{2}); (1;1; \frac{3}{2}; \frac{1}{2})$ . In an equivalent hybrid state the second vortex is shifted in phase by  $\pi$ . The particle flows of the in-phase and out-of-phase vortices are co-rotating, and hence the pair shares a singular vortex line at the center [Fig. 4 (a)]. In contrast, the hybrid vortex states are equivalent to interacting counter-rotating vortices. Their vortex lines have opposite charge and collide, producing two additional vortex lines splintering away from the interaction area [see Fig. 4 (b)], but conserving the total vortex charge. The algebra of these vortex lines and the exciting possibility of controlling their direction will be discussed elsewhere.

Stability of the planar vortex pairs depends critically on the coupling between vortices. We find no examples of stable out-of-phase co-rotating and the counter-rotating pairs, whereas the in-phase co-rotating vortices can be very robust. The in-phase configuration, due to the positive coupling between nearest-neighbor lobes, is equivalent to a  $\pi$ -phase jump between the wavefunctions, due to the nature of the linear Bloch waves. Such phase "twisting" has a stabilizing effect as previously discovered in the framework of discrete nonlinear systems with attractive nonlinearities [10]. The actual region of stability for the co-rotating vortex states depends on the strength of the coupling (which depends on the values of  $\gamma$  and  $V_0$ ), in agreement with the results for 2D vortices with an attractive nonlinearity [11]. The state shown in Fig. 4 (a) is dynamically stable to  $t = 10^3$ .

Most remarkably, we find that vortex "stacks" of multiple co-rotating vortices (somewhat analogous to the stacks of "pancakes" [12]), forming an extended discrete vortex line, can also be highly robust, in both the off-site [Fig. 5 (a)] and on-site configurations [Fig. 5 (b)]. These results demonstrate that a 3D optical lattice can provide transverse stabilization of vortex lines. This effect can be explored experimentally, since without the transverse periodicity, vortex lines exhibit strong "snake-type" instabilities [12]. The possibility of long wavelength modula-

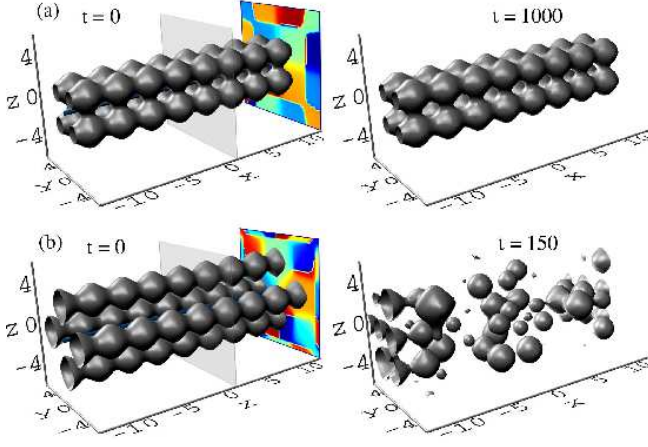


FIG. 5: (color online) Example of a stable o-site vortex stack at  $t = 0$  (a) and at  $t = 10^3$  (b) ( $\gamma = 7:9$ ). (c) Unstable on-site vortex stack at  $t = 0$  and  $t = 150$  ( $\gamma = 7:5$ ) (d).

tional instability can not be ruled out however, especially at long time scales [13]. Our numerical simulations performed with stacks up to 16 lattice sites long have found no trace of such an instability at  $t = 10^3$  [Fig. 5(a)]. When the instability is present, e.g. due to stronger inter-lobe coupling, it develops rapidly, leading to the spectacular "explosion" of the vortex line [see Fig. 5(b)].

Apart from the generalizations of planar 2D gap vortices, 3D lattices can support vortices which have no 2D analogs. The "truly" 3D vortex with the strongest coupling between lobes is the four-site state with simple phases  $(0; \frac{1}{2}; 1; \frac{3}{2})$  (in multiples of  $\pi$ ) shown in Fig. 6(b). We term this configuration a "folded vortex", which can be viewed as a combination of two dipoles  $(0; 1)$  and  $(\frac{1}{2}; \frac{3}{2})$  that are not equivalent in inter-site coupling strengths. Similar coupling structure also occurs for a planar rhomboid vortex [9]. The simplest fully symmetric 3D vortex is that of the out-of-plane coupled dipole state of Fig. 6(c). As can be seen by the particle flow arrows, the vortex circulation is highly nontrivial.

Fully 3D lattices also offer us the possibility of combining different symmetry elements of 2D vortex states. The simplest example is the "vortex diamond" shown in Fig. 6(d), which consists of two coupled planar vortices lying in the orthogonal symmetry planes. Unlike the incoherently coupled out-of-plane vortices [4], this is a coherent fully 3D vortex characterized by a single chemical potential, and it can not be reduced to 2D equivalents.

A remarkable feature of the uniquely 3D gap vortices is their dynamical stability up to at least  $t = 10^3$  for a range of chemical potentials and lattice depths which is much broader than that of the bound states of two or more planar vortices. The experimental generation of these states is an open problem. However they appear to be an extremely robust means of introducing localized vorticity into the 3D lattice.

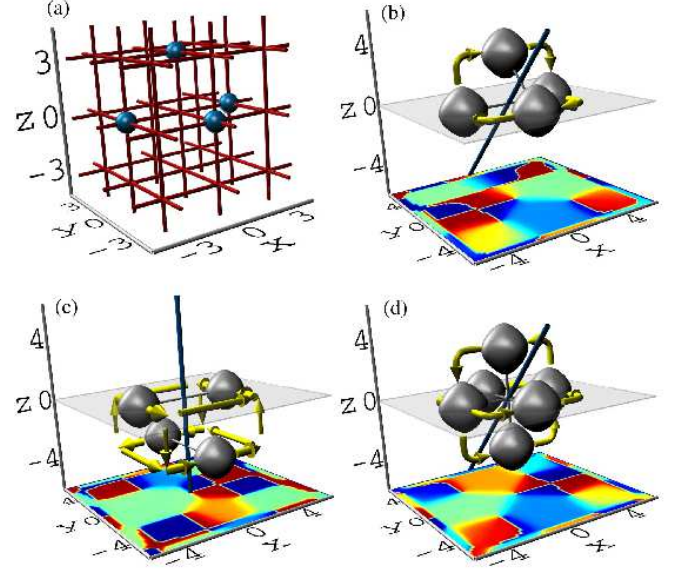


FIG. 6: (color online) Novel 3D vortices at  $V_0 = 6$ ,  $\gamma = 7:9$ . (a) Folded vortex shown in (b) relative to the positions of the lattice in (a). (c) Crossed-dipole vortex and (d) vortex diamond. Thick lines correspond to the primary vortex lines.

In conclusion, we have predicted novel classes of spatially localized vortex structures in BECs loaded into 3D optical lattices. Such structures include planar vortices, vortex stacks, folded vortices and vortex diamonds. We have demonstrated numerically that many of these vortex structures are remarkably robust, and therefore they may be generated and observed in experiment. Our results open up the possibility of studying more complex condensate structures such as localized vortex rings and knots in periodic potentials.

- 
- [1] W. Thompson, Phil. Mag. 34, 15 (1897).
  - [2] J. R. Anglin and W. Ketterle, Nature 416, 211 (2002).
  - [3] E. A. Ostrovskaya and Yu. S. Kivshar, Phys. Rev. Lett. 93, 160405 (2004).
  - [4] P. G. Kevrekidis et al., Phys. Rev. Lett. 93, 080403 (2004).
  - [5] M. Greiner et al., Nature 415, 39 (2002).
  - [6] O. Zobay et al., Phys. Rev. A 59, 643 (1999); P. J. Louis et al., Phys. Rev. A 67, 013602 (2003); B. Eiermann et al., Phys. Rev. Lett. 92, 230401 (2004); V. Ahuñger et al., Phys. Rev. A 69, 053604 (2004).
  - [7] J. J. Garcia-Ripoll and V. M. Perez-García, SIAM J. Sci. Comput. 23, 1316 (2001).
  - [8] H. Pu et al., Phys. Rev. A 67, 043605 (2003).
  - [9] T. J. Alexander et al., Phys. Rev. Lett. 93, 063901 (2004).
  - [10] Yu. Kivshar, M. Peyrard, Phys. Rev. A 46, 3198 (1992).
  - [11] J. K. Yang, New J. Phys. 6, 47 (2004).
  - [12] J. P. Martikainen, H. T. C. Stoof, Phys. Rev. Lett. 93, 070402 (2004).
  - [13] S. Damanyan et al., Phys. Rev. B 59, 5994 (1999).